Published in final edited form as:
Biochemistry. 2007 August 14; 46(32): 9174–9186. doi:10.1021/bi7002058.

Expanding the Repertoire of an ERK2 Recruitment Site: Cysteine Footprinting Identifies the D-Recruitment Site as a Mediator of Ets-1 Binding†

Olga Abramczyk[‡], **Mark A. Rainey**[§], **Richard Barnes**[‖], **Lance Martin**[⊥], and **Kevin N. Dalby**[*,‡,§,‖]

[‡] Division of Medicinal Chemistry, University of Texas at Austin, Texas 78712

[§] Graduate Program in Molecular Biology, University of Texas at Austin, Texas 78712

[‖] Graduate Program in Biochemistry, University of Texas at Austin, Texas 78712

[⊥] Department of Biochemistry, Stanford University, Stanford, California 94305

Abstract

Many substrates of ERK2 contain a D-site, a sequence recognized by ERK2 that is used to promote catalysis. Despite lacking a canonical D-site, the substrate Ets-1 is displaced from ERK2 by peptides containing one. This suggests that Ets-1 may contain a novel or cryptic D-site. To investigate this possibility a protein footprinting strategy was developed to elucidate ERK2–ligand interactions. Using this approach, single cysteine reporters were placed in the D-recruitment site (DRS) of ERK2 and the resulting ERK2 proteins subjected to alkylation by iodoacetamide. The ability of residues 1–138 of Ets-1 to protect the cysteines from alkylation was determined. The pattern of protection observed is consistent with Ets-1 occupying a hydrophobic binding site within the DRS of ERK2. Significantly, a peptide derived from the D-site of Elk-1, which is known to bind the DRS, exhibits a similar pattern of cysteine protection. This analysis expands the repertoire of the DRS on ERK2 and suggests that other targeting sequences remain to be identified. Furthermore, cysteine-footprinting is presented as a useful way to interrogate protein–ligand interactions at the resolution of a single amino acid.

The mitogen-activated protein kinases (MAPKs)[1] are ubiquitous elements of eukaryotic signaling pathways that permeate nearly all aspects of signaling in multicellular organisms. In humans the loss of their regulation is associated with many diseases that encompass an expanding list of cancers as well as neurological and inflammatory diseases (1). Three main subgroups have been identified in humans, termed the ERKs (2), the JNKs (3,4), and the p38 MAPKs (5,6). Several newer members have recently been reviewed (7). Extracellular regulated protein kinase 2 (ERK2), the prototypical member of the MAP kinase family, catalyzes the

†This research was supported in part by the Welch Foundation (F-1390) and the National Institutes of Health (GM59802). Mass spectra were acquired by Dr. Herng-Hsiang Lo in the CRED Analytical Instrumentation Facility Core supported by the NIEHS center grant ES07784. Molecular graphics images were produced using the UCSF Chimera package from the Resource for Biocomputing, Visualization, and Informatics at the University of California, San Francisco (supported by NIH P41 RR-01081).

[*] Corresponding author. Division of Medicinal Chemistry, College of Pharmacy, University of Texas at Austin, TX 78712. Tel: 512-4719267. Fax: 512-2322606. Dalby@mail.utexas.edu..

SUPPORTING INFORMATION AVAILABLE

Tables of DNA primers used for the generation of mutants. This material is available free of charge via the Internet at http://pubs.acs.org.

transfer of the γ-phosphate of adenosine triphosphate to serine or threonine residues that generally lie in flexible regions of proteins. It is a remarkable enzyme whose ability to exhibit high specificity toward a discrete subset of structurally diverse proteins is poorly understood.

Protein kinases generally recognize substrates through a consensus sequence that contains the phosphorylation site (8). This sequence is recognized, in part, by a region called the activation segment that encompasses residues ^{165}DFG to APE^{195} of the catalytic domain of protein kinases (9) (See Figure 1A, red). As most protein kinases are able to phosphorylate peptides that correspond to consensus sequences with reasonable efficiency, mechanistic and structural studies have mainly focused on peptides and consequently those specificity factors that are intrinsic to the consensus sequence of a substrate (8,10). However, protein substrates are usually phosphorylated with higher specificity constants than peptide substrates, reflecting the opportunity available to proteins to make additional interactions with a protein kinase that are extrinsic to this sequence (10). MAPKs are an extreme example, because they employ recruiting sites that bind discrete docking sites[2] on substrates that are extrinsic to the consensus sequence (11-13).

An important recruitment site that mediates catalytic substrate interactions is the D-recruitment site (DRS), which contains a hydrophobic groove on the rear face of ERK2, formed by three structural elements: the α_D *helix–loop-8–*α_E *helix* and the β_7 *sheet–loop-11–*β_8 *sheet* segments provide important hydrophobic interactions, while *loop-16* makes important polar contributions (Figure 1B). The DRS of ERK2 recognizes a D-site either with the sequence of $(R/K)_{2–3}$-$X_{4–6}$-Φ_A-X-Φ_B (in this sequence X represents any amino acid and Φ = Leu, Ile, or Val) or a related sequence found in MAPKAP kinases (11). The structures of several D-sites bound to the DRSs of the three major MAPK classes (p38 MAPK (13), JNK (14), and ERK2 (15, 16)) have been reported. These structures reveal a common, *but not uniform*, mode of binding where the characteristic basic residues engage acidic residues on loop-16, while the Φ residues bind to hydrophobic sites (indicated by Ø) within the groove (See Figures 2A and 2B which depicts two D-sites bound to ERK2 (15, 16)).

To address fundamental questions relating to the mechanism of ERK2 we have utilized the recombinant N-terminal hexahistidine fusion protein, EtsΔ138, which is composed of residues 1–138 of the transcription factor Ets-1, an excellent surrogate for the full-length protein (17) (Figure 1C). Two regions characterize this protein: a five-helix bundle called the *pointed* (PNT) domain and an unstructured highly flexible N-terminus, which contains Thr-38, the sole ERK2 phosphorylation site (18,19).

Mechanistic studies have established that, in the presence of MgATP and excess Mg^{2+}, ERK2 phosphorylates EtsΔ138 exclusively on Thr-38 to a stoichiometry of 1 mol/mol with a specificity constant of $k_{cat}/K_m = 2 \times 10^6\ M^{-1}\ s^{-1}$ (17). Steady-state kinetic studies are consistent

[1]Abbreviations: 5-IAF, 5′-iodoacetomido-fluorescein; BSA, bovine serum albumin fraction V; DTNB, 5,5′-dithiobis(2-nitrobenzoic acid); DTT, dithiothreitol; EDTA, ethylene diamine tetraacetic acid; EGTA, ethylene glycerol-bis[2-aminoethyl ether]-*N*,*N*,*N*′,*N*′-tetraacetic acid; IAA, iodoacetamide; PMSF, phenylmethanesulfonyl fluoride; TPCK, tosylphenylalanylchloromethane; NTCB, 2-nitro-5-thiocyanobenzoic acid; HEPES, *N*-(2-hydroxyethyl)-piperazine-*N*′-2-ethanesulfonic acid; IPTG, isopropyl-*β*-D-thiogalactopyranoside; ERK, extracellular signal-regulated protein kinase; EtsΔ138, murine (His$_6$-tagged)Ets1(1–138); MAPK, mitogen-activated protein kinase; MAPKAP, mitogen-activated protein kinase activated protein kinase; MKK1, MAP kinase kinase 1; MKP-3, MAP kinase phosphatase 3; PKA, protein kinase A; JNK, c-Jun kinase; ERK2-*CT*, an ERK2 protein containing a single cysteine target residue as well as a C-terminal PKA consensus sequence; TIM, triosephosphate isomerase; PCR, polymerase chain reaction; ESI, electrospray ionization; k_a, the observed second-order rate constant for the alkylation of ERK2-*CTs* under native conditions; k'_a, the observed second-order rate constant for the alkylation of ERK2-*CTs* under native conditions in the presence of saturating ligand; CD site, common docking site, usually designated as Asp-316 and Asp-319 of loop-16 (rat ERK2 numbering); DRS, D-recruitment site; FRS, F-recruitment site.

[2]Two docking sites have been identified on MAPK ligands. One is called a D-site and is recognized by the D-recruitment site (DRS). The other is called an F-site and is recognized by the F-recruitment site (FRS). D-sites have also been called DEJL-domains, while F-sites have also been called DEF domains or Phe-X-Phe domains.

with the notion that ERK2 phosphorylates EtsΔ138 through a random-order ternary-complex mechanism (20), and pre-steady-state burst experiments revealed two partially rate-limiting enzymatic steps, which have rate constants of $k_2 = 109 \pm 9\ s^{-1}$ and $k_3 = 56 \pm 4\ s^{-1}$ (21). These steps were attributed to the phosphorylation of bound EtsΔ138, k_2, and processes associated with product release, k_3, respectively. Recently, evidence was provided for the existence of two ternary complexes on the reaction pathway, prior to the phosphorylation step (22). It was proposed that one ternary complex is stabilized exclusively by interactions extrinsic to the consensus sequence and that this ternary complex can interconvert to a less stable ternary complex in which the consensus sequence of Ets-1 intimately engages the active site. This was termed a proximity-induced mechanism of catalysis, highlighting the catalytic role extrinsic docking interactions play in increasing the concentration of the consensus sequence within the proximity of the active site (22).

A structural basis for understanding the proximity-induced mechanism is currently lacking. While Ets-1 does not appear to contain a conventional docking motif, two regions of Ets-1 are known to interact with ERK2 (23). The first, which corresponds to the sequence ^{110}**K**ECF**L**E**L**APDF^{120}, is found within the PNT domain (in Figure 1C, Phe-120 is highlighted) (19). Although this sequence conforms, in part, to the consensus sequence for a D-site, mutagenesis data suggests that the interaction of this site with ERK2 is primarily mediated by the hydrophobic residue Phe-120, which lies in the $\Phi_B + 4$ position, a position not previously noted as being important for the binding of ligands to the DRS of ERK2. Binding studies also indicate that a second site of interaction lies in the highly flexible N-terminus, although this site has not yet been located (23).

Despite lacking a canonical D-site, the substrate Ets-1 is displaced from ERK2 by peptides containing a D-site (23). This suggests that Ets-1 may contain a novel or cryptic D-site. To investigate this possibility a cysteine footprinting strategy was developed to elucidate ERK2–ligand interactions. Using this approach, single cysteine residues were placed in the DRS of a form of ERK2 that had been engineered to be free of other cysteines and which contained a C-terminal protein kinase A phosphorylation site for radioactive labeling. The resulting proteins, termed ERK2-cysteine targets (ERK2-*CTs*) were subjected to alkylation by iodoacetamide. The ability of Ets-1, as well as a peptide derived from the D-site of Elk-1, to protect the ERK2-*CTs* from alkylation was determined. The similar footprinting/protection patterns induced by both ligands suggest that they occupy the same hydrophobic binding site within the DRS of ERK2.

EXPERIMENTAL PROCEDURES

Reagents

Ammonium hydroxide and TCA (trichloroacetic acid) were purchased from Fisher Scientific (Pittsburgh, PA). Ultrapure grade Tris was obtained from ICN Biomedicals (Aurora, OH). Sodium bicine, IAA (iodoacetamide), sodium deoxycholate, NTCB (2-nitro-5-thiocyanobenzoic acid), guanidine, catalytic subunit of protein kinase A, and other chemicals were obtained from Sigma (St. Louis, MO). MP Biomedicals (Irvine, CA) supplied [γ-^{32}P]-ATP. Yeast extract, tryptone, agar, and IPTG were obtained from US Biologicals (Swampscott, MA). Qiagen Inc. (Valencia, CA) supplied Ni-NTA agarose, Quiaprep Spin miniprep, PCR QIAquick Purification Kit, and QIAEX II Gel Extraction Kit. Restriction enzymes, PCR reagents, and T4 DNa ligase were from New England Bioloabs (Beverly, MA) and Invitrogen Corp. (Carlsbad, CA). Oligonucleotides for DNA amplification and mutagenesis were from Genosys (Woodlands, TX). Mutagenesis reagents were purchased from Stratagene (La Jolla, CA). Ambion, Inc. (Austin, TX), provided the thin walled PCR tubes. The Mono Q HR 10/10 anion exchange column and PD-10 desalting columns were purchased from Amersham Biosciences (Piscataway, NJ). *Escherichia coli* strain DH5α, used for cloning and mutagenesis,

and strains BL21 (DE3) and BL21(DE3)pLys, used for recombinant protein expression, were obtained from Invitrogen and Novagen (Madison, WI), respectively. pET28a vector was purchased from Novagen.

General Methods

Techniques for restriction enzyme digestion, ligation, transformation, and other standard molecular biology manipulations were based on methods described by the manufacturer. Plasmids were introduced into cells using a BTX Transporter Plus. UV–vis absorbance readings were taken on a Varian Cary model 50 spectrophotometer. FPLC was performed on a Pharmacia ÄKTA FPLC system. HPLC was performed on a Waters HPLC system using a 250 mm × 4 mm Vydac RP C18 column (218TP54, reversed-phase material consists of octadecyl aliphatic groups bonded to the surface of 300 Å pore diameter silica). Protein was analyzed by Tris glycine sodium dodecyl sulfate–polyacrylamide gel electrophoresis (SDS–PAGE) under denaturing conditions on 10–15% gels using the Bio-Rad Mini-protean III vertical gel electrophoresis apparatus. The extinction coefficients (ε) for ERK2 and Ets-1 proteins were determined by first measuring the concentration of a protein solution by amino acid analysis and then, where necessary, correcting for mutations in the primary sequence, according to $\varepsilon = 5690\ cm^{-1}\ M^{-1} \times$ (number of trp) + $1280\ cm^{-1}\ M^{-1} \times$ (number of tyr) + $120\ cm^{-1}\ M^{-1} \times$ (number of cys) (24). All mutants were verified by sequencing the DNA at UT core facilities using an Applied Biosystems automatic DNA sequencer.

Molecular Biology

PCR Conditions—PCR was carried out in a Techne Genius Thermal Cycler (Techne Inc., Princeton, NJ). The amplification reactions (100 μL) contained standard *Taq* amplification buffer, 200 μM each of the four deoxynucleoside triphosphates, 0.5 μM primers, 5 ng of template DNA, 1.5 mM $MgCl_2$, and 0.5 U of *Taq* DNA polymerase. Typical cycling parameters were 94 °C for 5 min, followed by 30 cycles at 55 °C for 30 s, 72 °C for 1 min, and 94 °C for 45 s with a final elongation step of 72 °C for 10 min.

Construction of ERK2 Mutants for Kinetic Studies—NpT7-5 His_6-ERK2 was digested with *Sac*II and *Hin*dIII and ligated into a *Sac*II–*Hin*dIII digested pBluescript (pBS) vector using T4 DNA ligase to create pBS-ERK2. This was modified by PCR using site-directed mutagenesis to generate the following construct D316A/D319A ERK2. The first round of PCR generated two overlapping products, fragments A and B, from two separate reactions using pBS-ERK2 as template. Fragment A was amplified using an outer forward primer that contained an *Eco*RI restriction site and an inner reverse primer containing a mutation. Fragment B was amplified with an inner forward primer containing the same mutation and an outer reverse primer containing an *Hin*dIII restriction site. Fragments A and B were purified and used as templates for a second round of PCR using only the outer primers, A and B. The product was digested with *Eco*RI and *Hin*dIII and ligated into *Eco*RI–*Hin*dIII digested pBS-ERK2. The pBS-ERK2 mutants were digested with *Sac*II and *Hin*dIII and subcloned into *Sac*II–*Hin*dIII digested NpT7-5 His_6-ERK2. Mutants containing two mutations were made using single mutant DNA as template and incorporating a second mutation. Construction of L113A, Q117A, and H123A ERK2 mutants were carried out in a similar manner to above using different outside primers and restriction enzymes.

Construction of pET28-His_6-ERK2cysless-PKA—A mutant of ERK2 lacking cysteines, ERK2 C125S/C159S/C252L/C63A/C38A/C164A/C214A (amino acid numbering corresponds to protein from cDNA of wild type *Rattus norvegicus* ERK2; GenBank accession number M64300) was created using several steps of the overlap extension polymerase chain reaction using the appropriate primers and pBluscript–ERK2 DNA as a template. Mutants were introduced serially using the previous DNA mutant as a template. The ERK2 cysteineless

mutant DNA was then digested from the Bluescript vector with *Sac*II and *Hin*dIII and subcloned into NpT7-5 between the corresponding restriction sites *Sac*II and *Hin*dIII to create NpT7-5 His_6-ERK2 C125S/C159S/C252L/C63A/C38A/C164A/C214A. The DNA from the NpT7-5 His_6-ERK2 C125S/C159S/C252L/C63A/C38A/C164A/C214A vector was then used as a template, and the PCR product was amplified using a forward and reverse primer. The forward primer contains a hexahistidine tag, and the reverse primer contains a sequence encoding a C-terminal tag corresponding to amino acids Gly-Arg–Arg-Ala-Ser-Ile-Tyr that is recognized by PKA. The PCR product was digested, purified, and ligated into pET28 at *Nco*I and *Hin*dIII sites to give *pET28-His_6-ERK2cysless-PKA.*

Construction of Cysteine Reporters in the DRS of pET28-His_6-ERK2cysless-PKA—Single cysteine mutants of ERK2 were generated by PCR according to the standard procedure of the QuickChange site directed mutagenesis kit (Strategene) using pET28-His_6-ERK2cysless-PKA construct as a template. All amplification reactions (50 μL) contained PfuUltra HF polymerase buffer, 200 μM each of the four deoxynucleoside triphosphatases, 10 ng of template DNA, 150 ng of primers forward and reverse, 2.5 U of PfuUltra HF polymerase (Stratagene). The cycling parameters were 94 °C for 30 s, followed by 16 cycles at 56 °C for 1 min, 68 °C for 7 min, 94 °C for 30 s with a final elongation step 68 °C for 10 min. Digestion of template DNA was performed for 4 h using *Dpn*I. Reaction mixtures (10 μL) were transformed into *E. coli* DH5α following the method of Hanahah et al. (25).

Construction of Cysteine Free EtsΔ138—A pET 28a bacterial expression vector encoding a hexahistidine tag followed by a thrombin cleavage site and cDNA encoding murine Ets1 residues 1–138 (pET28a-EtsΔ138 was a gift of L. P. McIntosh, University of British Columbia, Vancouver) was modified by overlap extension polymerase chain reaction to construct the cysteine-less mutant of EtsΔ138 (*C31A/C99A/C106A/C112A*) in an EtsΔ138 S26A background as reported elsewhere (23).

Expression and Purification of Proteins

(i) EtsΔ138 Proteins: EtsΔ138—Residues 1–138 of murine Ets-1 cDNA (with Ser26 substituted for Ala) were expressed as an N-terminal hexahistidine fusion protein in *E. coli* BL21 (DE3) as described previously (17). *His_6-EtsΔ138 C31A/C99A/C106A/C112A.* The protein was expressed in BL21(DE3)pLys *E. coli* cells and purified according to the methods described previously (17).

(ii) ERK2 Proteins: Inactive Rat ERK2—This was expressed in *E. coli* BL21 (DE3), purified, and activated as described previously (21). *His_6-ERK2 Single Cysteine PKA-Tagged Mutants.* All ERK2 single cysteine constructs were electroporated into BL21(DE3) *E. coli* cells. Cells were grown at 37 °C in Luria broth containing 30 μg/mL kanamycin to an optical density of 0.8 and then were inducted with 0.5 mM IPTG for 4 h at 30 °C. The cells were harvested, lysed in buffer A (40 mM Tris pH 7.5, 0.03% (by mass) Brij-30, 0.1% (v/v) β-mercaptoethanol, 1 mM benzamidine, 0.1 mM PMSF, and 0.1 mM TPCK) containing 0.75 M NaCl and 1% (by mass) Triton X-100, and sonicated for 20 min at 4 °C (at 5 s pulses with 5 s intervals). The lysate was cleared and the supernatant was agitated with Ni-NTA beads for 1 h at 4 °C. After washing the beads with 150 mL of buffer A containing 10 mM imidazole the His_6-tagged proteins were eluted with 50 mL buffer A (pH 8.0) containing 200 mM imidazole. The eluted proteins were applied to a Mono Q HR 10/10 anion exchange column equilibrated in buffer B (20 mM Tris pH 8.0, (v/v) 0.03% Brij-30, (v/v) 0.1% β-mercaptoethanol). The column was developed over 15–17 column volumes with a linear gradient of 0–0.5 M NaCl. Fractions of single cysteine ERK2 mutants, eluted at 220–250 mM NaCl were collected and dialyzed into buffer (25 mM HEPES pH 7.5, 50 mM KCl, 0.1 mM EDTA, 0.1 mM EGTA, 2 mM DTT, 10% glycerol). The concentration was established using the extinction coefficient

(A_{280}) of 52067 cm^{-1} M^{-1} for wild type ERK2 and then correcting for cysteines as described above.

His_6-tag Cleavage—His_6-EtsΔ138 cysteine-less mutant expressed from pET 28a has an N-terminal sequence of Met-Gly-Ser-Ser-His-His-His-His-His-His-Ser-Ser-Gly-Leu-Val-Pro-Arg-Gly-Ser-His prior to the initial methionine encoded by the EtsΔ138 cDNA. To remove the hexahistidine tag, His_6-EtsΔ138 C31A/C99A/C106A/C112A (30 mg) was subjected to thrombin cleavage in 30 mL reaction volume containing 10 units of thrombin. The cleavage was carried out for 5 h at 25 °C in cleavage buffer (20 mM Tris, 150 mM NaCl, and 2.5 mM $CaCl_2$). The reaction sample was dialyzed in buffer B containing 0.1 mM EDTA, 0.1 mM EGTA at 4 °C and applied to a Mono Q HR 10/10 anion exchange chromatography. Collected fractions were combined and dialyzed into buffer (25 mM HEPES, pH 7.5, 50 mM KCl, 0.1 mM EDTA, 0.1 mM EGTA 2 mM DTT). Cleavage of the His_6-tag was confirmed by SDS-PAGE and mass spectrometry. The concentration was established using an extinction coefficient (A_{280}) of 22760 for EtsΔ138 C31A/C99A/C106A/C112A. Proteins and tryptic peptides were analyzed by an electrospray ion trap mass spectrometer (LCQ, Finnigan MAT, San Jose, CA) coupled on-line with a microbore HPLC (Magic 2002, Michrom BioResources, Auburn, CA) as described elsewhere (21).

Enzyme Kinetics

Steady-State Kinetics—Assay conditions were 25 mM Hepes, pH 7.5, 50 mM KCl, 0.1 mM EDTA, 0.1 mM EGTA, 40 μg/mL BSA, 20 mM $MgCl_2$, 2 mM DTT, ERK2, and ATP. Previous experiments had determined that double reciprocal plots of 1/*v*versus 1/[EtsΔ138] or 1/[$MgATP^{2-}$] are linear and display a pattern of intersecting lines below the abscissa at a common vertical coordinate (20). This is typical of a sequential mechanism where both substrates react before either dissociates from the enzyme. It was assumed that the perturbation of the enzyme–substrate interactions would not substantially alter the mechanism. Kinetic experiments were typically performed a minimum of two times for each mutant.

Cysteine Alkylation Kinetics

His_6-ERK2 containing a single cysteine and a C-terminal PKA site (30–50 μg) was radiolabeled for 15 min at 37 °C in 50 mM Tris, pH 7.5, 10 mM $MgCl_2$, 1 U of catalytic subunit of protein kinase A, 4 mM DTT, 1 μM unlabeled ATP, and 10 μCi of [γ-^{32}P]-ATP (7000 Ci/mmol). The enzymatic activity of the PKA was quenched by the addition of 5 μM PKI, a potent inhibitor of PKA (26). The radiolabeled ERK2 (20 μg, 2.6 μM) was then incubated in the presence or absence of a ligand (either 2.3 mM EtsΔ138 lacking cysteines and the His tag, or 1 mM D-site peptide QKGRKPRDLELPLSPSL) in 180 μL buffer (25 mM HEPES pH 7.5, 50 mM KCl, 40 μg/mL BSA, 2 mM DTT, 0.1 mM EDTA, 0.1 mM EGTA, 1.3% glycerol) at 27 °C. After 30 min this solution was diluted 1.6-fold into a solution containing iodoacetamide (0.8–16 mM; final concentrations) and sodium bicine (160 mM) and incubated at 23 °C and pH 8.3. Aliquots (30 μL) were taken at various time points and quenched with an equal volume of quench solution (40 mM β-mercapthoethanol and 0.1 mg/mL BSA). Alkylated samples were stored at −20 °C or immediately denatured and cleaved using NTCB. For alkylation reactions conducted in the presence of a high concentration of EtsΔ138, the EtsΔ138 was removed by first binding the ERK2 to Ni-NTA agarose beads (50 μL) that had been equilibrated in 50 mM KH_2PO_4 pH 7.5, and 100 mM NaCl for 20 min and then washing the resin with 5 mL of Ni-binding buffer. The ERK2 mutant was then eluted from the beads using 50 mM KH_2-PO_4, 100 mM NaCl, and 50 mM EDTA pH 8.0 (100 μL). The recovered ERK2 was denatured by the addition of an equal volume of 8 M guanidine HCl, 200 mM sodium bicine pH 8.6 and incubated for 15 min at 23 °C. The exposed sulfhydryl group of cysteine in the denatured ERK2 was then subjected to cyanylation by incubating with NTCB (25 mM) for 15 min at 23 °C (27,28). The ERK2 was then precipitated by the addition of 0.05% sodium deoxycholate and 50% trichloroacetic acid

(29). The sample was then centrifuged for 20 min at 14000*g*, and the pellets were washed twice with 500 μL acetone, dried (speed vac), and then resuspended in 20 μL of 8 M urea and 0.6 M NH_4OH to initiate polypeptide cleavage. After the cleavage reaction was complete (1 h at 37 °C), the ammonia was allowed to evaporate. After the addition of loading dye (5 μL), the radioactivity of each sample was counted using a Packard 1500 scintillation counter to facilitate the addition of equal quantities of protein to a 15% or 20% SDS–PAGE gel. The proteins were then fractionated and the gels dried using a Gel Dryer (Biorad) before being exposed on image plates (Amersham Pharmacia) for 0.5–12 h. The gels were quantified using a PhosphorImager (Molecular Dynamics) and analyzed using ImageQuant software (30,31). Data obtained from the gel analysis were fitted to a first-order decay curve and generally found to reproducible to within 20%.

Peptide Synthesis and Purification

A peptide derived from Elk1: QKGRKPRDLELPLSPSL (1934 Da) that contains a D-site (consensus underlined) (32), was synthesized at the UT Molecular Biology core facilities. The crude peptide was dissolved in equilibration buffer (0.1% trifluoroacetic acid) and purified by reverse phase chromatography using an Econosil C18 column (Alltech), developed with linear acetonitrile gradient 0–100% over 90 min using a flow rate 5 mL/min. Fractions absorbing at 280 nm were collected and lyophilized. The peptide was resuspended in water and the pH raised to 7.5 by the addition of sodium hydroxide. The concentration of the peptide was determined by amino acid analysis, and the molecular weight of the peptide was estimated by MALDI mass spectrometry.

RESULTS AND DISCUSSION

Recently, the D-site peptide QKGRKPRDLELPLSPSL derived from Elk-1, which binds the DRS of ERK2, was shown to displace Ets-1 from *both* the activated and unactivated forms of ERK2 (23). We hypothesized that rather than displacing Ets-1 through an allosteric mechanism this peptide directly competes with Ets-1 for the DRS of ERK2. The basis for this hypothesis was the observation that the structural transitions that accompany the binding of a D-site peptide to the DRS of ERK2 (15,16) are very similar to those that occur upon the conversion of ERK2 from the unactivated to the activated form upon MKK1-mediated phosphorylation (33). Thus, we reasoned that, if Ets-1 binds both major conformations of ERK2, the most likely explanation that the D-site peptide displaces Ets-1 from ERK2 is that it occupies part of the Ets-1 binding site.

To examine this hypothesis we decided to use a cysteine footprinting approach. When the alkylation rates of cysteine residues present in native protein structures (v_a) are compared to the alkylation rates of the same cysteines in denatured proteins ($v°_a$), a 10^5-fold range in the ratio of $v°_a/v_a$ is observed (34). This range of reactivity has been described using a model which assumes that a rapid equilibrium (k_1/k_{-1}) (between a solvent inaccessible folded state **I** and solvent accessible exposed states **II**) precedes cysteine alkylation, k_{alk} (Scheme 1) (35). According to this model, only the exposed states **II** are reactive and therefore if the equilibrium, k_1/k_{-1}, is fast compared to k_{alk} the observed rate constant for alkylation, k_a, is given by $k_a = k_1/k_{-1})k_{alk}$ (34,35). Typically, little variation in k_{alk} is expected, suggesting that the magnitude of k_1/k_{-1} usually determines cysteine reactivity. This is supported by the correlation between k_a and solvent accessibility that holds over a reactivity range of 5 orders of magnitude (31). We reasoned that cysteine residues placed within the DRS of ERK2 would serve to report the engagement of ligands at this locus through a decrease in their observed rate of alkylation. A related approach has been used to predict the TIP47 protein binding site for the mannose 6-phosphate receptor (30), as well as the substrate binding site of TIM (34). While ligand binding has the potential to increase or decrease k_1/k_{-1}, and hence affect the reactivity of an ERK2-

CT, by inducing a conformational change of a side chain or backbone segment, the relative inflexibility of the DRS suggests that for cysteines within the DRS a ligand-induced change in reactivity is likely to be the direct consequence of binding and not a conformational change (see the discussion below).

Preparation of ERK2-Single Cysteine Targets (ERK2-CTs)

To perform the cysteine footprinting on ERK2, all of the cysteines were conservatively mutated by site-directed mutagenesis to produce ERK2 with the following seven amino acid substitutions: C38A, C63A, C125S, C159S, C164A, C214A, and C252L. Incorporation of a C-terminal extension, GRRASIY, allowed ERK2 to be specifically phosphorylated at the C-terminus by protein kinase A (PKA). The ability to unambiguously label ERK2 at one of its termini is critical for the cysteine footprinting assay (Scheme 2 shows the chemical basis for the cysteine footprinting). The DNA encoding this modified enzyme was then subcloned into pET28a to incorporate an N-terminal hexahistidine tag into the protein, which provides a convenient method of isolating the ERK2 from excess ligand during the workup of the footprinting assay (see Experimental Procedures). The unactivated ERK2 mutant was expressed in *E. coli* and purified following a similar protocol used for the wild type enzyme (21) and after *in vitro* activation by a constitutively active form of MKK1 and further purification, it was assayed. It was found to be highly active, exhibiting steady-state kinetic parameters of $k_{cat} = 6.2 \pm 0.6\ s^{-1}$ and $K_m = 51 \pm 11\ \mu M$, for the phosphorylation of EtsΔ138. These values compare favorably to the kinetic parameters for the wild type enzyme ($k_{cat} = 20\ s^{-1}$, $K_m = 20\ \mu M$), suggesting that the cysteine residues play a minimal role in substrate binding and catalysis. Importantly, these values suggest that cysteine-free ERK2 could be used to investigate interactions between ERK2 and its cognate ligands.

Choice of Cysteine Targets—Using the complex of ERK2, bound to the D-site peptide RLQERRGSNVALMLDV from hematopoietic protein tyrosine phosphatase as the reference structure (16), several ERK2-*CTs* were chosen (See Table 1 and Figure 2). This structure reveals two hydrophobic sites termed $Ø_1$ and $Ø_2$, which engage the $Φ_A$-X-$Φ_B$ motif (LML) of the peptide. ERK2-*CTs* Cys-123, -126, and -159 were designed to investigate binding to the $Ø_1$ site (it should be noted that Cys-159 is present in the wild type sequence of ERK2). ERK2-*CTs* Cys-113, -117, -119, -155, -123, and -159 were designed to investigate binding to the $Ø_2$ site. In addition to the hydrophobic interactions, basic residues within D-sites are frequently thought to interact with the common docking (CD) site in loop-16 (Asp-316 and Asp-319), therefore ERK2-*CTs* Cys-316 and -319 were also prepared. The ERK2-*CTs* were expressed and purified to homogeneity before being specifically labeled at the C-terminus by incubating with protein kinase A, using [γ-^{32}P]-ATP.

Footprinting Reveals Binding of Ets-1 and a D-Site Peptide in the DRS of ERK2

Kinetics—To test whether EtsΔ138 binds the DRS of ERK2, ERK2-*CT*s were alkylated with IAA in the absence and presence of EtsΔ138 and the rate constant for ERK2-*CT* alkylation was determined by using an NTCB-mediated cleavage protocol to differentiate alkylated from unalkylated ERK2-*CT* (34). Figure 3 shows a typical set of SDS—PAGE gels used to fractionate NTCB-mediated cleavage reactions. These were performed at different times after the initiation of ERK2-*CT* alkylation, as indicated above each lane. The slower running band (*) in each lane corresponds to the uncleaved proteins **I** or **III** (see Scheme 2), which result from either alkylation (**I**) or β-elimination (**III**) of the cyanylated protein **II**.[3] The faster running band in each lane (**IV**) (cleaved as indicated) corresponds to the C-terminal half of the cleaved

[3]A major side reaction of **II**, under the cleavage conditions employed, is the β-elimination to give **III**, the rate of which is sensitive to the amino acid sequence and can account for as much as 50% of the reaction in some of the experiments reported (27). In addition, a relatively low level of nonspecific cleavage also occurs throughout the protein.

protein. To quantify alkylation, the intensity of a quadrant containing **IV** was determined *relative* to a quadrant encompassing the entire lane. This approach allowed for any variability in sample loading and background radioactivity between lanes. The relative density of each gel quadrant was found to be reproducible to within 20% between experiments after normalizing for the variability seen in the background radioactivity between experiments. In some cases a trace amount of **IV** was apparent after exhaustive incubation with IAA (see lanes labeled Inf). This likely reflects a small fraction of misfolded protein in the preparation that is resistant to alkylation by IAA, but which can still be cleaved by NTCB under denaturing conditions. The disappearance of **IV** corresponds to ERK2-*CT* alkylation. In all the cases that were examined the alkylation of ERK2-*CTs* by excess IAA was found to follow a pseudo-first-order rate law (see Figure 4 for some examples). The second-order rate constants for alkylation derived from these and similar plots were found to be in the range of 0.035–18 M^{-1} s^{-1}, depending on which mutant was examined (Table 1). Each experiment was performed a minimum of two times using different ERK2-*CT* preparations. The second-order rate constants were found to be reproducible to within 30% and are reported in Table 1. The sensitivity and reproducibility of the footprinting analysis is such that a 2-fold difference in a rate constant for alkylation may be determined readily.

Ets-1 Binding—To examine the degree to which the substrate EtsΔ138 protects each ERK2-*CT*, the alkylation reactions were performed under conditions where the concentration of EtsΔ138 exceeds the dissociation constant for the ERK2·EtsΔ138 complex by more than 50-fold. Several ERK2-*CTs*, Q117C, L113C, L119C, and H123C, were found to exhibit protection (3–7-fold) when in the presence of a saturating concentration of EtsΔ138. In contrast, the reactivity of several other ERK2-*CTs* were unaffected by the binding of EtsΔ138 (See Table 1). In no case was the reactivity of an ERK2-*CT* toward IAA increased as might be expected if a conformational change occurred in the DRS. All the protected ERK2-*CTs* contain a cysteine in the $Ø_2$ site (see residues highlighted in yellow in Figure 5A), consistent with the notion that $Ø_2$ is an Ets-1 binding site.

Peptide Binding—Although the footprinting experiments suggested that Ets-1 binds the DRS, it was important to compare these experiments to those using a reference D-site peptide that was known to bind this site (36). Previously, QKGRKPRDLELPLSPSL, which is derived from Elk-1, had been shown by HX-MS studies to bind the DRS of ERK2 (36). Figure 6 shows several SDS–PAGE gels used to fractionate NTCB-mediated cleavage products of ERK2-*CTs* after alkylation in the absence and presence of a saturating concentration (625 μM) of the D-site peptide. Quantification of these and other gels, in the same manner as described above for EtsΔ138, furnished pseudo-first-order progress curves (see Figure 7 for some examples), which were used to determine second-order rate constants for alkylation. Four ERK2-*CTs*, Cys-113, Cys-117, Cys-155, and Cys-159, were found to exhibit protection (2–33-fold), while several others, Cys-119, Cys-123, Cys-126, Cys-316, and Cys-319, exhibited no protection (Table 1). While the absence of protection by the peptide may result from the lack of ERK2-*CT* binding, we consider this to be unlikely given the high concentration of peptide used in the experiments. As in the experiments with EtsΔ138, no ERK2-*CT* exhibited an increased reactivity upon peptide binding.

Significantly, the cysteines that exhibit sensitivity to the binding of the peptide are also concentrated near the $Ø_2$ site (See Figure 5B), and in all cases except Cys-159, the magnitude of their protection is also in the range of 3–6-fold (Table 1 and Figure 8). Given that the peptide is known to bind the DRS, these observations support the notion that direct protection is being detected in both cases. As the wild type amino acid at position 159 is cysteine, Cys-159 has the potential to interact intimately with a naturally evolved ligand for ERK2. This might explain why ERK2-*CT* Cys-159 is protected more effectively by the peptide than other ERK2-*CTs*. It should be noted that the protection patterns for both the peptide and EtsΔ138 do not rule out

the possibility that they interact with the $Ø_1$ binding site, because this site is flanked by Cys-159, which also flanks the $Ø_2$ site. As the $Ø_2$ site can accommodate several different hydrophobic amino acid side chains, presumably with varying degrees of intimacy, it is not surprising that EtsΔ138 and the peptide induce different degrees of protection. These differences probably reflect alternative ligand binding modes (see Figure 8 and Table 1 for a comparison of the protection patterns). In fact, the binding modes of the two D-site peptides in Figure 2 are clearly not the same, which translate to differences in how they interact with the residues in the $Ø_2$ site. For example peptide RLQERRGSNVALMLDV (Figure 2B) interacts more closely with loop-8 compared to peptide RRLKQGNLPVR (Figure 2A), which interacts more closely with loop-11. The absence of any protection of Y126C (RE), L155C (L11), and C159 (L11) by EtsΔ138 suggests that it also binds closer to loop-8 than loop-11. The absence of protection of D316C and D319C (the CD-site) by EtsΔ138 is consistent with the notion that Ets-1 does not interact with this site. The steady-state parameters for the phosphorylation of EtsΔ138 by the D316A/D319A mutant also support this view (Table 2).

Although the peptide and Ets-1 exhibit similar protection patterns within the DRS (both magnitude and location), an allosteric mechanism must be considered as a possible reason for the observed protection by both the peptide and Ets-1. An allosteric mechanism requires that the binding of the ligand induces a conformational change within the DRS that leads to localized cysteine protection. However, an analysis of the path traced by the backbone atoms of the DRS reveals only minor deviations between three forms of ERK2 (unactivated, activated, and unactivated in complex with a D-site peptide) (Figure 5C), suggesting that conformational changes in the DRS are probably not sufficient to support such a mechanism. Furthermore, these deviations are uniform throughout the site and do not reveal a localized conformational change that could potentially lead to the selective protection of cysteines that are seen upon peptide and EtsΔ138 binding.

Comparison of Cysteine Footprinting with Mutagenesis and HX-MS

The HX-MS approach may be used to reveal areas of solvent protection by analyzing the rate of H/X exchange into exchangeable backbone hydrogens (37). Cysteine footprinting may be used to reveal areas of solvent protection by analyzing the reactivity of specifically positioned cysteines. Each approach provides an analysis of solvent accessibility that reflects the structure and dynamics of a protein and can be used to provide information on changes in protein environment associated with ligand binding. These techniques represent complementary approaches that may be of particular use when interrogating protein–protein interactions where high-resolution crystal or NMR structures are unavailable. While the resolution of the HX-MS approach is limited to peptide fragments, it has the advantage of allowing a large fraction of a protein to be scanned relatively easily. In the case of ERK2, for example, it was possible to analyze almost 90% of the molecule (36). Thus, HX-MS provides the opportunity for wide coverage, but at a relatively low resolution. In contrast, the cysteine footprinting approach described here provides narrow coverage, but at the resolution of a single amino acid. An analysis termed misincorporation protein-alkyl exchange (MPAX), which utilizes the misincorporation of cysteine residues into proteins through the use of mutant t-RNAs, is an interesting methodology that potentially expands the footprinting approach by encompassing the advantages of both approaches (31). More studies are required to compare the ability of each approach to accurately define a protein–ligand interaction.

To determine the importance of some of the residues in the DRS for binding and catalysis, the corresponding alanine mutants were prepared and analyzed kinetically (Table 2). With the exception of H123A, all the mutants tested demonstrated kinetic properties that were within 2-fold of the wild type protein. The essentially wild type parameters exhibited by the D316A/D319A double mutant are consistent with the absence of protection seen for the ERK2-*CTs*

D316C and D319C. Taken together, these results suggest that the ERK2 common docking (CD) site does not participate in the interface formed by the ERK2·Ets-1 complex. The basis for the slightly higher k_{cat} and K_m of the H123A mutation on the catalytic parameters of ERK2 is unclear. An evaluation of the effects of this mutation on individual steps of the catalytic mechanism, using a transient kinetic approach (20), will be informative and interesting. The insensitivity of the catalytic parameters to the alanine mutants of Leu-113 and Gln-117, which contribute to the ERK2·EtsΔ138 interface, highlights the difficulties of using alanine scanning experiments to define protein–protein interactions.

CONCLUSION

The DRS is a critical locus on ERK2 for the recognition of protein substrates. To date, all proteins known to be recruited by this site contain the D-site motif $(R/K)_{2–3}$-$X_{4–6}$-Φ_A-X-Φ_B (Φ = Leu, Ile, or Val), or a poorly defined, but related, site found in the C-terminus of the MAPKAPs (11). Despite lacking an obvious motif for DRS recognition, the transcription factor Ets-1 is efficiently phosphorylated by ERK2 and is shown here to interact with it. Thus, Ets-1 may contain a novel or cryptic D-site, which resides either in the PNT domain or in its flexible N-terminus. Identifying this site is important to understand the basis for the mechanism of proximity-induced catalysis exhibited by ERK2 (22).

Supplementary Material

Refer to Web version on PubMed Central for supplementary material.

Acknowledgments

We are indebted to Dr. Melanie Cobb (UT Southwestern Medical Center) and Dr. Natalie G. Ahn (University of Colorado at Boulder) for generously providing us with DNA encoding His_6-ERK2 and His_6-MKK1G7B, respectively. We also thank the reviewers for excellent suggestions.

REFERENCES

1. Pearson G, Robinson F, Beers Gibson T, Xu BE, Karandikar M, Berman K, Cobb MH. Mitogen-activated protein (MAP) kinase pathways: regulation and physiological functions. Endocr. Rev 2001;22:153–183. [PubMed: 11294822]
2. Cobb MH, Robbins DJ, Boulton TG. ERKs, extracellular signal-regulated MAP-2 kinases. Curr. Opin. Cell Biol Dec;1991 3:1025–1032. [PubMed: 1667578]
3. Derijard B, Hibi M, Wu IH, Barrett T, Su B, Deng T, Karin M, Davis RJ. JNK1: a protein kinase stimulated by UV light and Ha-Ras that binds and phosphorylates the c-Jun activation domain. Cell 1994;76:1025–1037. [PubMed: 8137421]
4. Kyriakis JM, Banerjee P, Nikolakaki E, Dai T, Rubie EA, Ahmad MF, Avruch J, Woodgett JR. The stress-activated protein kinase subfamily of c-Jun kinases. Nature 1994;369:156–160. [PubMed: 8177321]
5. Lee JC, Laydon JT, McDonnell PC, Gallagher TF, Kumar S, Green D, McNulty D, Blumenthal MJ, Heys JR, Landvatter SW, et al. A protein kinase involved in the regulation of inflammatory cytokine biosynthesis. Nature Dec 22–29;1994 372:739–746. [PubMed: 7997261]
6. Han J, Lee JD, Bibbs L, Ulevitch RJ. A MAP kinase targeted by endotoxin and hyperosmolarity in mammalian cells. Science Aug 5;1994 265:808–811. [PubMed: 7914033]
7. Bogoyevitch MA, Court NW. Counting on mitogen-activated protein kinasess—ERKs 3, 4, 5, 6, 7 and 8. Cell. Signalling 2004;16:1345–1354. [PubMed: 15381250]
8. Kemp BE, Parker MW, Hu S, Tiganis T, House C. Substrate and pseudosubstrate interactions with protein kinases: determinants of specificity. Trends Biochem. Sci 1994;19:440–444. [PubMed: 7855883]

9. Nolen B, Taylor S, Ghosh G. Regulation of protein kinases; controlling activity through activation segment conformation. Mol. Cell 2004;15:661–675. [PubMed: 15350212]
10. Fujii K, Zhu G, Liu Y, Hallam J, Chen L, Herrero J, Shaw S. Kinase peptide specificity: improved determination and relevance to protein phosphorylation. Proc. Natl. Acad. Sci. U.S.A 2004;101:13744–13749. [PubMed: 15356339]
11. Sharrocks AD, Yang SH, Galanis A. Docking domains and substrate-specificity determination for MAP kinases. Trends Biochem. Sci 2000;25:448–453. [PubMed: 10973059]
12. Gum RJ, Young PR. Identification of two distinct regions of p38 MAPK required for substrate binding and phosphorylation. Biochem. Biophys. Res. Commun 1999;266:284–289. [PubMed: 10581204]
13. Chang CI, Xu BE, Akella R, Cobb MH, Goldsmith EJ. Crystal structures of MAP kinase p38 complexed to the docking sites on its nuclear substrate MEF2A and activator MKK3b. Mol. Cell 2002;9:1241–1249. [PubMed: 12086621]
14. Heo YS, Kim SK, Seo CI, Kim YK, Sung BJ, Lee HS, Lee JI, Park SY, Kim JH, Hwang KY, Hyun YL, Jeon YH, Ro S, Cho JM, Lee TG, Yang CH. Structural basis for the selective inhibition of JNK1 by the scaffolding protein JIP1 and SP600125. EMBO J 2004;23:2185–2195. [PubMed: 15141161]
15. Liu S, Sun JP, Zhou B, Zhang ZY. Structural basis of docking interactions between ERK2 and MAP kinase phosphatase 3. Proc. Natl. Acad. Sci. U.S.A 2006;103:5326–5331. [PubMed: 16567630]
16. Zhou T, Sun L, Humphreys J, Goldsmith EJ. Docking interactions induce exposure of activation loop in the MAP kinase ERK2. Structure 2006;14:1011–1019. [PubMed: 16765894]
17. Waas WF, Dalby KN. Purification of a model substrate for transcription factor phosphorylation by ERK2. Protein Expression Purif 2001;23:191–197.
18. Slupsky CM, Gentile LN, Donaldson LW, Mackereth CD, Seidel JJ, Graves BJ, McIntosh LP. Structure of the Ets-1 pointed domain and mitogen-activated protein kinase phosphorylation site. Proc. Natl. Acad. Sci. U.S.A 1998;95:12129–12134. [PubMed: 9770451]
19. Seidel JJ, Graves BJ. An ERK2 docking site in the Pointed domain distinguishes a subset of ETS transcription factors. Genes Dev 2002;16:127–137. [PubMed: 11782450]
20. Waas WF, Dalby KN. Transient protein-protein interactions and a random-ordered kinetic mechanism for the phosphorylation of a transcription factor by extracellular-regulated protein kinase 2. J. Biol. Chem 2002;277:12532–12540. [PubMed: 11812784]
21. Waas WF, Rainey MA, Szafranska AE, Dalby KN. Two rate-limiting steps in the kinetic mechanism of the serine/threonine specific protein kinase ERK2: a case of fast phosphorylation followed by fast product release. Biochemistry 2003;42:12273–12286. [PubMed: 14567689]
22. Rainey MA, Callaway K, Barnes R, Wilson B, Dalby KN. Proximity-Induced Catalysis by the Protein Kinase ERK2. J. Am. Chem. Soc 2005;127:10494–10495. [PubMed: 16045329]
23. Callaway KA, Rainey MA, Riggs AF, Abramczyk O, Dalby KN. Properties and Regulation of a Transiently Assembled ERK2.Ets-1 Signaling Complex. Biochemistry 2006;45:13719–13733. [PubMed: 17105191]
24. Gill SC, von Hippel PH. Calculation of protein extinction coefficients from amino acid sequence data. Anal. Biochem 1989;182:319–326. [PubMed: 2610349]
25. Hanahan D, Jessee J, Bloom FR. Plasmid transformation of Escherichia coli and other bacteria. Methods Enzymol 1991;204:63–113. [PubMed: 1943786]
26. Walsh DA, Ashby CD, Gonzalez C, Calkins D, Fischer EH. Krebs EG: Purification and characterization of a protein inhibitor of adenosine 3′,5′-monophosphate-dependent protein kinases. J. Biol. Chem 1971;246:1977–1985. [PubMed: 4324557]
27. Tang HY, Speicher DW. Identification of alternative products and optimization of 2-nitro-5-thiocyanatobenzoic acid cyanylation and cleavage at cysteine residues. Anal. Biochem 2004;334:48–61. [PubMed: 15464952]
28. Wu J, Watson JT. Optimization of the cleavage reaction for cyanylated cysteinyl proteins for efficient and simplified mass mapping. Anal. Biochem 1998;258:268–276. [PubMed: 9570840]
29. Arnold U, Ulbrich-Hofmann R. Quantitative protein precipitation from guanidine hydrochloride-containing solutions by sodium deoxycholate/trichloroacetic acid. Anal. Biochem 1999;271:197–199. [PubMed: 10419639]
30. Burguete AS, Harbury PB, Pfeffer SR. In vitro selection and prediction of TIP47 protein-interaction interfaces. Nat. Methods 2004;1:55–60. [PubMed: 15782153]

31. Silverman JA, Harbury PB. Rapid mapping of protein structure, interactions, and ligand binding by misincorporation proton-alkyl exchange. J. Biol. Chem 2002;277:30968–30975. [PubMed: 12185208]

32. Yang SH, Whitmarsh AJ, Davis RJ, Sharrocks AD. Differential targeting of MAP kinases to the ETS-domain transcription factor Elk-1. EMBO J 1998;17:1740–1749. [PubMed: 9501095]

33. Canagarajah BJ, Khokhlatchev A, Cobb MH, Goldsmith EJ. Activation mechanism of the MAP kinase ERK2 by dual phosphorylation. Cell 1997;90:859–869. [PubMed: 9298898]

34. Silverman JA, Harbury PB. The equilibrium unfolding pathway of a (beta/alpha)8 barrel. J. Mol. Biol 2002;324:1031–1040. [PubMed: 12470957]

35. Feng Z, Butler MC, Alam SL, Loh SN. On the nature of conformational openings: native and unfolded-state hydrogen and thiol-disulfide exchange studies of ferric aquomyoglobin. J. Mol. Biol 2001;314:153–166. [PubMed: 11724540]

36. Lee T, Hoofnagle AN, Kabuyama Y, Stroud J, Min X, Goldsmith EJ, Chen L, Resing KA, Ahn NG. Docking motif interactions in MAP kinases revealed by hydrogen exchange mass spectrometry. Mol. Cell 2004;14:43–55. [PubMed: 15068802]

37. Engen JR. Analysis of protein complexes with hydrogen exchange and mass spectrometry. Analyst 2003;128:623–628. [PubMed: 12866878]

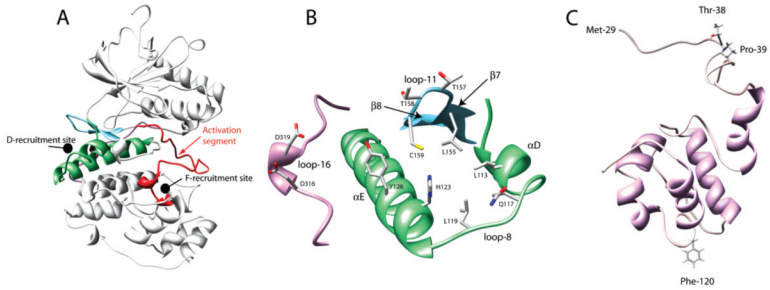

Figure 1.

Structure of EtsΔ138 and ERK2. A. Ribbon diagram of activated ERK2 (PDB 4ERK) showing the D-recruitment site (DRS) and the F-recruitment site (FRS). The activation segment (^{165}DFG–APE^{195}) is colored red. B. The DRS of ERK2 is composed of three segments: segment 1, helix αD–loop-8–helix αE (green); segment 2, strand β7–loop-11–strand β8 (cyan); and segment 3, loop-16 which contains the CD-site (Asp-316 and Asp-319) (plum). Several amino acids that have been shown to be important for recognition of various ERK2 ligands are indicated. C. A ribbon diagram depicting the NMR structure of Ets-1 (29–138) (PDB 1BQV) showing Thr-38 and Pro-39 in the flexible N-terminal tail, as well as Phe-120 in the PNT domain.

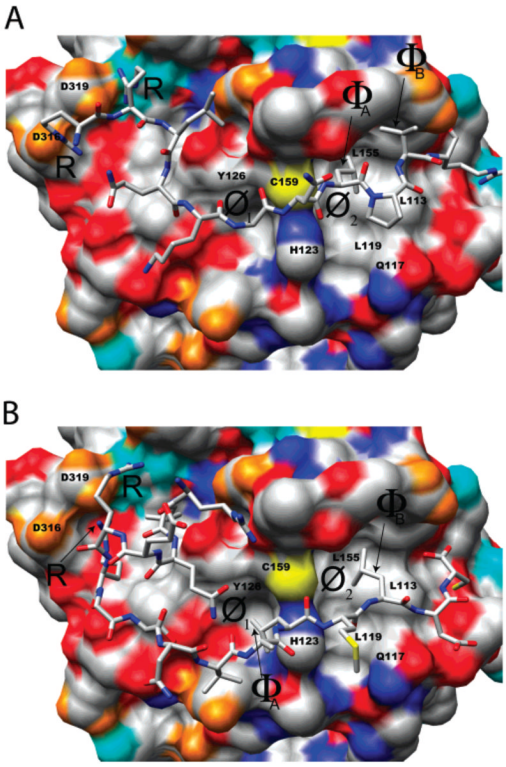

Figure 2.

Differences in the binding modes of D-site peptides to the DRS of ERK2. A. Binding of the D-site peptide RRLKQGNLPVR (consensus; $(R/K)_{2–3}$-$X_{4–6}$-Φ_A-X-Φ_B) derived from MAP kinase phosphatase-3 to unactivated ERK2. The Φ_A residue occupies the hydrophobic site $Ø_2$. B. The binding of the D-site peptide RLQERRGSNVALMLDV, derived from hematopoietic protein tyrosine phosphatase, to unactivated ERK2. The Φ_A and Φ_B residues of hematopoietic protein tyrosine phosphatase occupy the hydrophobic $Ø_1$ and $Ø_2$ sites, respectively. Surface representations: red, oxygen; orange, carboxylate oxygen; blue, neutral nitrogen; cyan, ε lysine nitrogen, or arginine guanidino nitrogen.

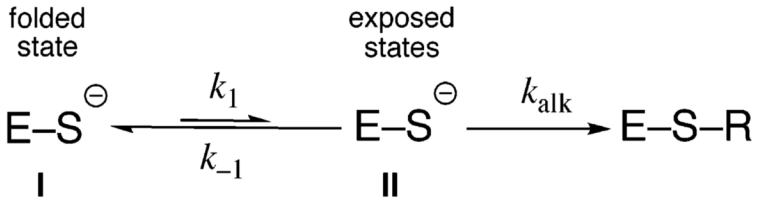

Scheme 1.
Model Describing an Equilibrium between the Folded State and Unfolded Exposed States That Determines the Rate of Cysteine Alkylation

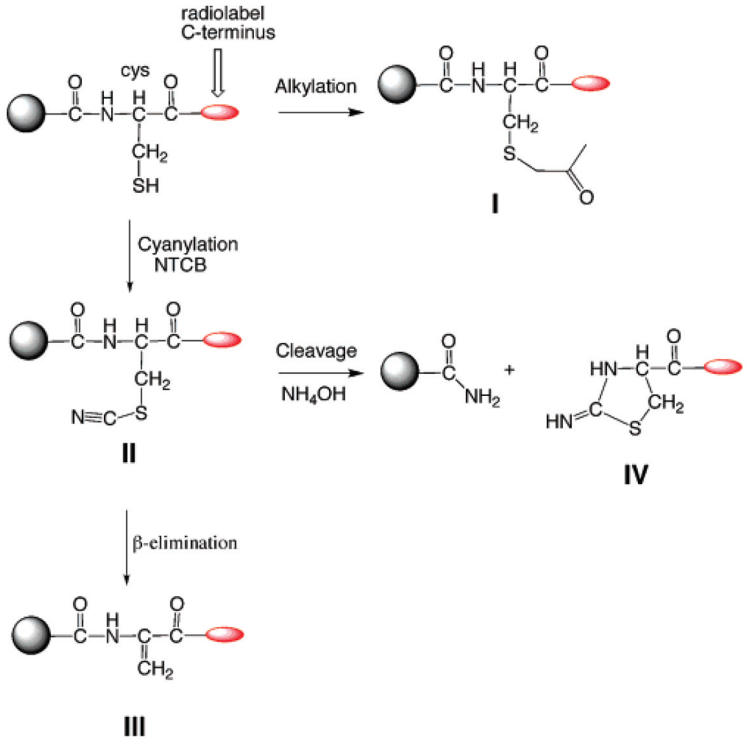

Scheme 2 a.

a ERK2 proteins containing single cysteine residues are incubated with iodoacetamide (IAA) to produce alkylated ERK2, **I**. Unalkylated ERK2 is cyanylated with NTCB to form the cyanylated intermediate **II**, which in the presence of ammonium hydroxide undergoes *β*-elimination to form **III** or polypeptide cleavage to form **IV**.

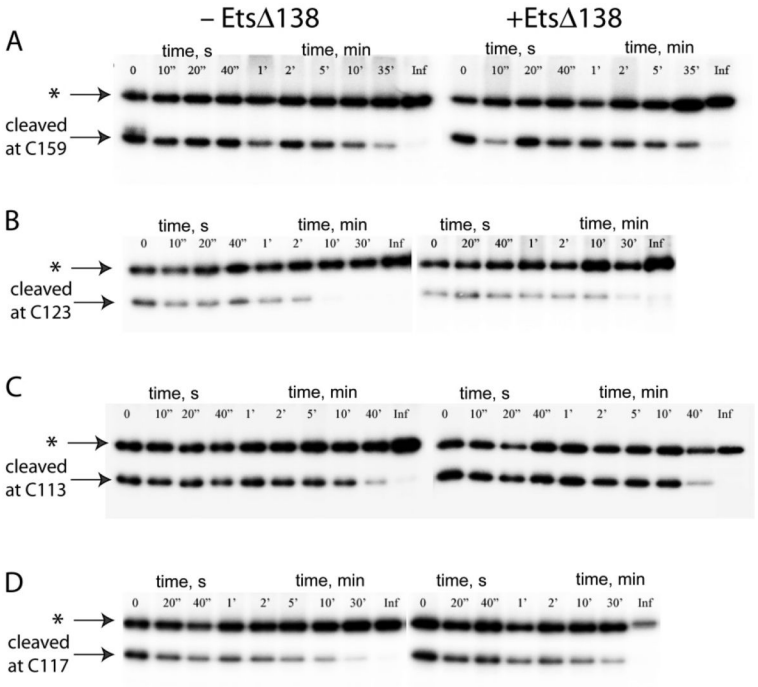

Figure 3.

Cysteine footprinting of the ERK2 and EtsΔ138·ERK2 complexes. C-terminally radiolabeled single cysteine ERK2 mutants (A, C159; B, H123C; C, L113C; and D, Q117C) were alkylated by iodoacetamide at pH 8.3 and 23 °C in the absence and presence of 1.45 mM EtsΔ138. At the times indicated above each lane, 30 μL aliquots were quenched with excess DTT, and the ERK2 was separated from excess EtsΔ138 (where necessary), denatured, and then cyanylated with excess (25 mM) 2-nitro-5-thiocyanobenzoic acid (NTCB). The cyanylated proteins were precipitated, washed, then resuspended and cleaved in 0.6 M NH_4OH. Samples were then fractionated by 15% SDS-PAGE, the gels dried, and the bands quantified on a Phosphorimager (see Experimental Procedures). The lanes correspond to the time when an aliquot was quenched. The upper band corresponds to uncleaved ERK2 (see **II** and **III** in Scheme 2), and the lower band corresponds to the fragment C-terminal to the single cysteine (**IV** in Scheme 2).

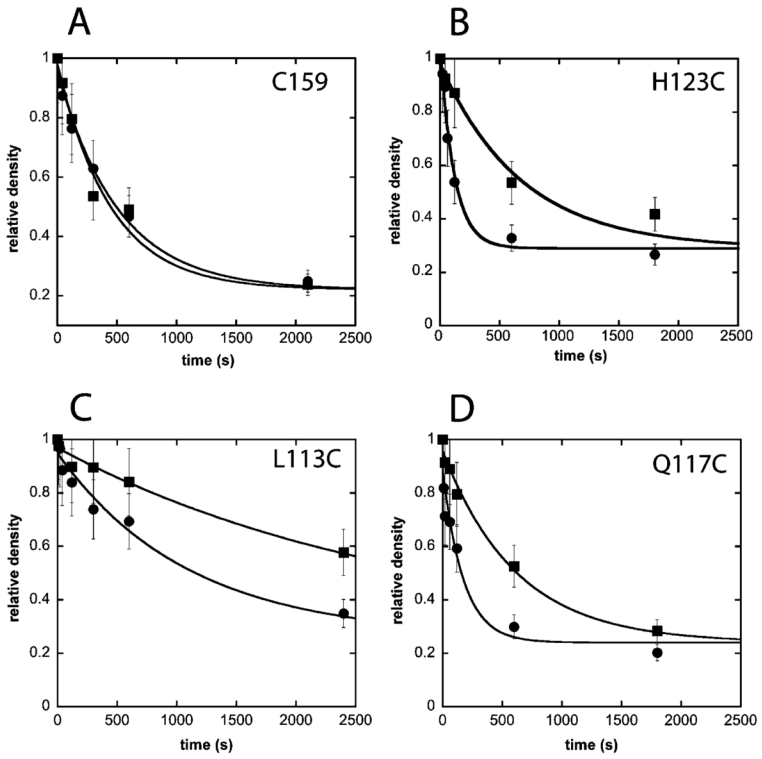

Figure 4.

Alkylation of ERK2-*CTs* versus time in the presence and absence of Ets¢138. Representative plots (A–D) showing the time course for the disappearance of unalkylated ERK2-*CTs* (measured by the presence of NTCB-mediated cleavage product) in the presence (●) and absence (■) of 1.45 mM EtsΔ138. The relative density of each gel quadrant (reproducible to within 20% after normalizing for variability in background radioactivity) containing a band associated with the ERK2-*CT* cleavage product was determined at various time points by phosphorimage analysis of gels similar to those shown in Figure 3 (see Experimental Procedures). The line through the data corresponds to the best fit to a first-order rate law (reproducible to within 30%). Endpoints used to determine rate constants for each alkylation reaction were determined after more than 10 half-lives. Some variability in the relative densities of the endpoints is seen between experiments, which mainly reflects variability in the background radioactivity of the gel quadrants used to determine the relative densities. Replicate experiments were performed on a minimum of two different preparations of each ERK2-*CT*. The sensitivity and reproducibility of the footprinting analysis is such that a 2-fold difference in a rate constant for alkylation may be readily determined. Rate constants and errors are reported in Table 1.

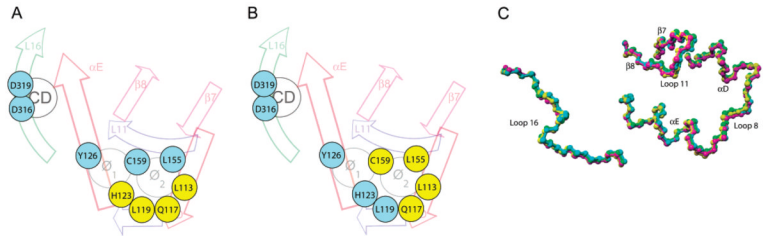

Figure 5.

Fooprinting patterns within the DRS exhibited by Ets-1 and a D-site peptide. A. Footprinting EtsΔ138. B. Footprining D-site peptide. Residues protected are shown in yellow circles, while those not protected are shown in blue circles. C. Alignment of DRS backbone residues for unactivated ERK2 (PDB 1ERK), activated ERK2 (PDB 2ERK), and unactivated ERK2 complexed to RRLQKGNLPVR (PDB 2FYS).

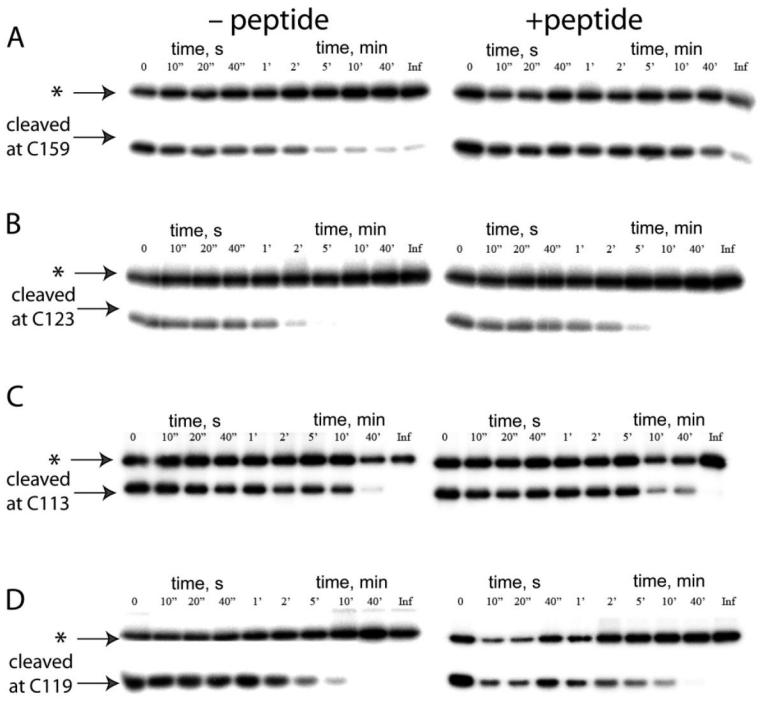

Figure 6.

Cysteine footprinting of a peptide·ERK2 complex. C-terminally radiolabeled single cysteine ERK2 mutants (A, C159; B, H123C; C, L113C; and D, L119C) were alkylated by iodoacetamide at pH 8.3 and 23 °C in the absence and presence of 0.625 mM peptide; QKGRKPRDLELPLSPSL. At the times indicated above each lane, 30 μL aliquots were quenched with excess DTT and the ERK2 was separated from excess EtsΔ138 (where necessary), denatured, and then cyanylated with excess (25 mM) 2-nitro-5-thiocyanobenzoic acid (NTCB). The cyanylated proteins were precipitated, washed, then resuspended and cleaved in 0.6 M NH_4OH. Samples were then fractionated by 15% SDS–PAGE, the gels dried, and the bands quantified on a Phosphorimager (see Experimental Procedures). The lanes correspond to the time when an aliquot was taken. The upper band corresponds to uncleaved ERK2 (see **II** and **III** in Scheme 2), and the lower band corresponds to the fragment C-terminal to the single cysteine (**IV** in Scheme 2).

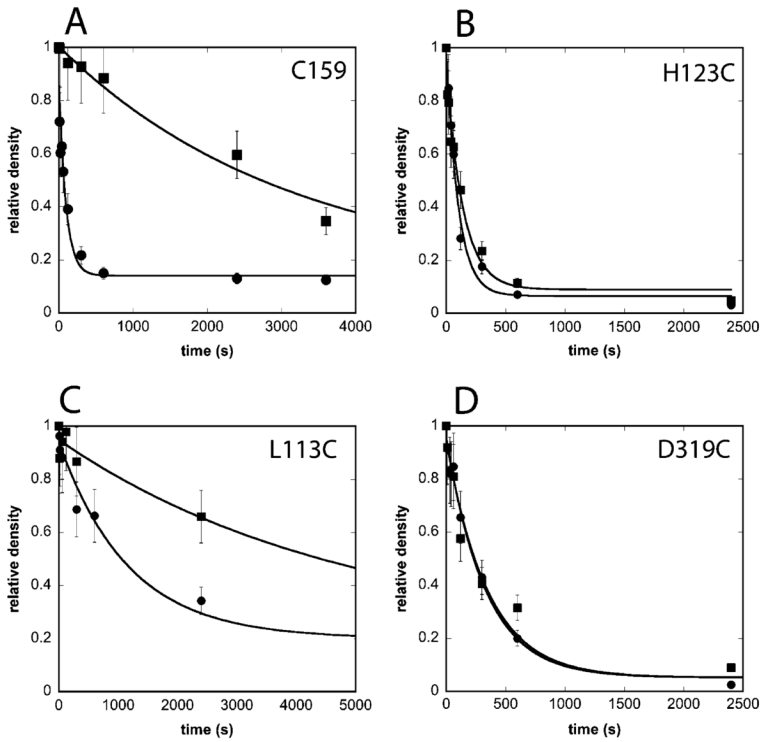

Figure 7.

Alkylation of ERK2-*CTs* versus time in the presence and absence of a D-site peptide. Representative plots (A–D) showing the time course for the disappearance of unalkylated ERK2-*CTs* (measured by the presence of NTCB-mediated cleavage product) in the presence (●) and absence (■) of 0.625 mM of peptide QKGRKPRDLELPLSPSL. The relative density of each gel quadrant (reproducible to within 20% after normalizing for variability in background radioactivity) containing a band associated with the ERK2-*CT* cleavage product was determined at various time points by phosphorimage analysis of gels similar to those shown in Figure 6 (see Experimental Procedures). The line through the data corresponds to the best fit to a first-order rate law (reproducible to within 30%). Endpoints used to determine rate constants for each alkylation reaction were determined after more than 10 half-lives. Some variability in the relative densities of the endpoints is seen between experiments, which mainly reflect variability in the background radioactivity of the gel quadrants used to determine the relative densities. Replicate experiments were performed on a minimum of two different preparations of each ERK2-*CT*. The sensitivity and reproducibility of the footprinting analysis are such that a 2-fold difference in a rate constant for alkylation may be readily determined. Rate constants and errors are reported in Table 1.

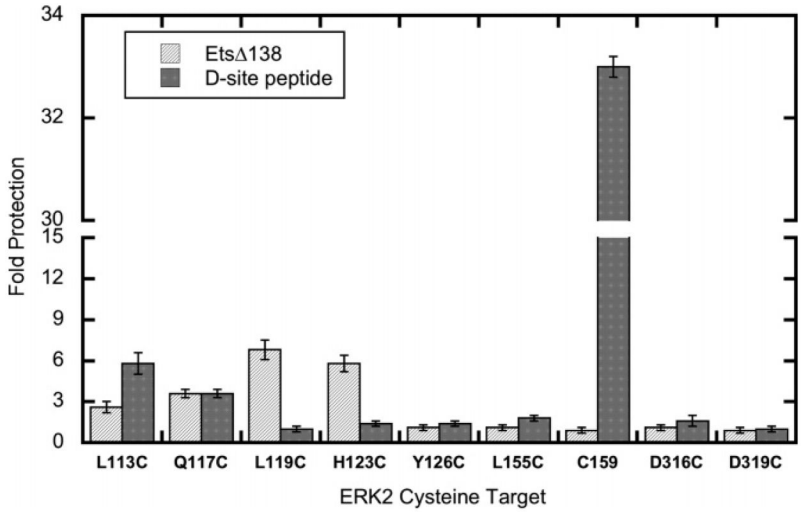

Figure 8.

Fold protection for the alkylation of ERK2-*CTs* by IAA in the presence of 0.625 mM QKGRKPRDLELPLSPSL or 1.45 mM EtsΔ138.

Table 1

Alkylation of ERK2-*CTs*

secondary structure	site[a]	cysteine	k_a[b] M^{-1} s^{-1}	fold protection k_a/k'_a peptide	fold protection k_a/k'_a EtsΔ138
αD helix	$Ø_2$	L113C	0.09 ± 0.01	5.8 ± 0.8	2.6 ± 0.4
loop-8	$Ø_2$	Q117C	6.5 ± 0.5	3.6 ± 0.3	3.6 ± 0.3
loop-8	$Ø_2$	L119C	0.65 ± 0.05	1.0 ± 0.2	6.8 ± 0.7
αE helix	$Ø_1$ and $Ø_2$	H123C	19.0 ± 1.0	1.4 ± 0.2	5.8 ± 0.6
αE helix	$Ø_1$	Y126C	2.1 ± 0.1	1.4 ± 0.2	1.1 ± 0.2
*β*7 sheet	$Ø_2$	L155C	0.04 ± 0.008	1.8 ± 0.2	1.1 ± 0.2
loop-11	$Ø_1$ and $Ø_2$	C159	1.8 ± 0.2	33.0 ± 4.0	0.9 ± 0.2
loop-16	CD[c]	D316C	0.6 ± 0.1	1.6 ± 0.4	1.1 ± 0.2
loop-16	CD[c]	D319C	0.5 ± 0.1	1.0 ± 0.2	0.9 ± 0.2

[a] The designation of the $Ø_1$ and $Ø_2$ binding pockets is based on the structure of RLQERRGSNVALMLDV (consensus; (R/K)$_{2–3}$-X$_{4–6}$-$Φ_A$-X-$Φ_B$, derived from hematopoietic protein tyrosine phosphatase, bound to unactivated ERK2 (16).

[b] Second-order rate constant for the alkylation of ERK2 mutants.

[c] CD site corresponds to Asp-316 and Asp-319 of rat ERK2.

Table 2

Kinetic Analysis of Mutations in the DRS on ERK2

secondary structure	location[a]	mutant ERK2	k_{cat} s^{-1}	K_m^{ets} 10^{-6} M	k_{cat}/K_m^{ets} 10^6 M^{-1} s^{-1}
		wild type	19.6 ± 0.7	8.8 ± 2.5	2.2
αD helix	Ø 2	L113A	22.0 ± 3.8	7.1 ± 2.4	3.0
loop-8	Ø 2	Q117A	18.0 ± 2.8	19.0 ± 3.0	1.0
αE helix	Ø 1	H123A	33.0 ± 2.9	43.0 ± 4.6	0.7
loop-16	CD[b]	D316A/D319A	18.0 ± 1.7	15.0 ± 3.2	1.1

[a] The designation of the $Ø_1$ and $Ø_2$ binding pockets is based on the structure of RLQERRGSNVALMLDV (consensus; $(R/K)_{2–3}$-$X_{4–6}$-$Φ_A$-X-$Φ_B$, derived from hematopoietic protein tyrosine phosphatase, bound to unactivated ERK2 (16).

[b] CD site corresponds to Asp-316 and Asp-319 of rat ERK2.